

Calculations of rotation-vibration states with the z axis perpendicular to the plane: High accuracy results for H 3 +

Maxim A. Kostin, Oleg L. Polyansky, and Jonathan Tennyson

Citation: The Journal of Chemical Physics 116, 7564 (2002); doi: 10.1063/1.1464540

View online: http://dx.doi.org/10.1063/1.1464540

View Table of Contents: http://scitation.aip.org/content/aip/journal/jcp/116/17?ver=pdfcov

Published by the AIP Publishing

Articles you may be interested in

Unraveling rotation-vibration mixing in highly fluxional molecules using diffusion Monte Carlo: Applications to H 3 + and H3O+

J. Chem. Phys. 136, 074101 (2012); 10.1063/1.3681391

The Al + – H 2 cation complex: Rotationally resolved infrared spectrum, potential energy surface, and rovibrational calculations

J. Chem. Phys. 127, 164310 (2007); 10.1063/1.2778422

Rotation-vibration states of H 3 + at dissociation

J. Chem. Phys. 118, 3538 (2003); 10.1063/1.1539034

Symmetry-adapted distributed approximating functionals: Theory and application to the ro-vibrational states of H 3 +

J. Chem. Phys. 110, 10283 (1999); 10.1063/1.478962

Ab initio calculation of the rotation–vibration energy levels of H 3 + and its isotopomers to spectroscopic accuracy J. Chem. Phys. **110**, 5056 (1999); 10.1063/1.478404



JOURNAL OF CHEMICAL PHYSICS VOLUME 116, NUMBER 17 1 MAY 2002

Calculations of rotation-vibration states with the z axis perpendicular to the plane: High accuracy results for H_3^+

Maxim A. Kostin, ^{a)} Oleg L. Polyansky, ^{a)} and Jonathan Tennyson ^{b)} Department of Physics and Astronomy, University College London, London WC1E 6BT, United Kingdon

(Received 3 December 2001; accepted 4 February 2002)

A method of calculation of rotation-vibration states for a general triatomic that places the body-fixed z axis perpendicular to the plane of the molecule is implemented within a discrete variable representation (DVR) for the vibrational motion. Calculations are presented for water and H_3^+ . For H_3^+ the new method improves on previous high accuracy ab initio treatments of the rotation-vibration energies of the molecule both in accuracy and the range of rotational states that can be treated. Reliable treatment of quasilinear geometries means that the method is also promising for treating very highly excited states. © 2002 American Institute of Physics. [DOI: 10.1063/1.1464540]

I. INTRODUCTION

The spectrum of H_3^+ has now been observed in a number of astrophysical locations 1 and is widely used as an observational handle on ionospheres of gas giant planets. 2 However, unraveling the laboratory spectrum of H_3^+ , a necessary precursor to the astrophysical studies has only been achieved with the aid of high-level *ab initio* calculations. $^{3-5}$

H₃⁺ is a two-electron system allowing electronic structure calculations of an accuracy unparalleled for any other polyatomic molecule.⁶ This has allowed a detailed exploration of effects usually ignored in the *ab initio* calculation of rotation–vibration spectra.^{6–10} However, even low-lying states of H₃⁺ undergo large-amplitude vibrational motion and it is therefore a challenging system for nuclear motion studies. There are now a number of reliable methods for calculating low-lying vibrational and rotational wave functions, but many of these have difficulty once the molecule begins to sample linear geometries. The barrier to linearity lies about 10 000 cm⁻¹ above the ground vibrational state, which means that the present spectroscopic studies are beginning to probe states that are influenced by linear geometries.¹¹

The most successful high-energy treatments of H_3^+ have, perhaps surprisingly, not utilized the full symmetry of the molecule. Studies that have exploited symmetry have focused on correctly including the permutation symmetry of the H atoms; see, for example, Refs. 18–20. However, for spectroscopic studies the correct treatment of rotational motion is of equal importance to the treatment of the vibrations. For H_3^+ the natural quantization axis for the rotations lies perpendicular to the plane of the molecule. In practice, detailed spectroscopic calculations have generally employed a z axis in the plane of the molecule. This is known to cause significant difficulties when the molecule samples linear geometries. 22

Sutcliffe and co-workers^{23,24} derived a generalized tri-

atomic nuclear motion Hamiltonian that has the *z* axis embedded perpendicular to the plane of the molecule. Sarkar *et al.*²⁵ showed how to avoid problems with singularities with this Hamiltonian, which they tested for the water molecule. There are better internal coordinate Hamiltonians available for treating the water problem.²⁶ In this work we present an implementation of this *z*-perpendicular Hamiltonian within the framework of our discrete variable representation (DVR) codes²⁷ and show that this form is a good one for studying H₃⁺, both from the perspective of high accuracy spectroscopic studies and for treating highly excited states, above the barrier to linearity. This suggests that this method should provide a useful starting point for treating rotational excitation in the near-dissociation region.¹⁷

II. THEORY

The Hamiltonian used here is expressed in Radau internal coordinates²⁸ that connect a distinct central atom with two identical other atoms. The body-fixed axis system places the z axis perpendicular to the plane of the molecule, the x axis bisects the Radau angle and the y axis is then chosen to make a right-handed set. The vibration—rotation kinetic energy operator (KEO) can be written as

$$T = T^{\text{vib}} + T^{\text{rot}} + T^{\text{cor}},\tag{1}$$

where (in atomic units)

$$T^{\text{vib}} = -\frac{1}{2m_1} \frac{\partial^2}{\partial R_1^2} - \frac{1}{2m_2} \frac{\partial^2}{\partial R_2^2} - \left(\frac{1}{2m_1 R_1^2} + \frac{1}{2m_1 R_2^2}\right) \frac{\partial}{\partial c} (1 - c^2) \frac{\partial}{\partial c}, \tag{2}$$

$$T^{\text{rot}} = \frac{1}{2} [G_{xx}J_x^2 + G_{yy}J_y^2 + G_{zz}J_z^2 + G_{xy}(J_xJ_y + J_yJ_x)], \quad (3)$$

$$T^{\text{cor}} = -\frac{i}{2} \left(G_{cz} \frac{\partial}{\partial c} + \frac{\partial}{\partial c} G_{cz} \right) J_z.$$
 (4)

a)Permanent address: Institute of Applied Physics, Russian Academy of Science, Uljanov Street 46, Nizhnii Novgorod, Russia 603950.

b) Electronic mail: j.tennyson@ucl.ac.uk

In these equations, R_1 , R_2 are the lengths of the two Radau vectors; $c = \cos(\theta)$ and θ is the angle between \mathbf{R}_1 and \mathbf{R}_2 , and J_x , J_y , J_z are standard rotational angular momenta operators. The nonzero elements of the \mathbf{G} matrix are given by

$$G_{cz} = (1 - c^2)^{1/2} M^-, (5)$$

$$G_{xx} = \frac{1}{1+c} M^+, (6)$$

$$G_{yy} = \frac{1}{1 - c} M^+, \tag{7}$$

$$G_{zz} = \frac{1}{2}M^+,\tag{8}$$

$$G_{xy} = -(1-c^2)^{-1/2}M^-, (9)$$

where

$$M^{\pm} = \frac{1}{2} \left(\frac{1}{m_1 R_1^2} \pm \frac{1}{m_2 R_2^2} \right). \tag{10}$$

This form of the Hamiltonian is as given by Sarkar *et al.*²⁵ However, we have checked that it is equivalent to those of Sutcliffe and co-workers, ^{23,24} who use a somewhat different notation.

Following Sarkar *et al.*²⁵ and to allow for correct behavior at linear geometries, Jacobi functions are used to represent the motions in the internal angle θ . These are given by

$$|j\rangle = h_{jab}^{-1/2} (1-c)^{a/2} (1+c)^{b/2} P_j^{ab}(c),$$
 (11)

where $h_{jab}^{-1/2}$ is a normalization constant and $P_{j}^{ab}(c)$ are Jacobi polynomials. As discussed further below, the choice,

$$a = b = \sqrt{\frac{1}{2}[J(J+1) - K^2]},$$
(12)

where J and K are the rotational angular momentum and its projection on the body-fixed z axis, ensures that the molecule behaves correctly at linear geometries.

To obtain real matrix elements with this Hamiltonian, it is necessary to transform the rotational matrix elements. The resulting rotational basis functions are²⁹

$$|JKq\rangle = \iota^{-q} \frac{\sqrt{2J+1}}{4\pi} [D_{K,M}^{J*} + (-1)^{K+q} D_{-K,M}^{J*}],$$

$$K > 0, \quad q = 0,1,$$

$$|JKq\rangle = \left(\frac{2J+1}{8\pi^2}\right)^{1/2} D_{K,M}^{J*}, \quad K = 0, \quad q = 0,$$
(13)

where $D_{K,M}^J$ (denoted $|JK\rangle$ below) is a rotation matrix.³⁰ With these functions, the rotational parity of the state is given by $(-1)^{J+K}$, and functions the symmetry with respect to interchange of the two identical atoms is given by $(-1)^{q+s}$, where s=0,1 and, as discussed below, represents the symmetry of the radial functions. For a given J, the Hamiltonian is therefore subdivided in four separate blocks according to the parity of K and q+s.²⁵ Figure 1 illustrates the structure of these four blocks.

Following the general procedure of Sutcliffe and co-workers, ^{23,24,31} we define an effective radial Hamiltonian by integrating the KEO's defined above over all angular co-

ordinates. Details of this procedure are given in the Appendix and only the final results are given below.

The effective vibrational KEO is diagonal in both the rotational and angular basis:

$$\langle JKqj|T^{\text{vib}}|JK'q'j'\rangle = \left(-\frac{1}{2m_1}\frac{\partial^2}{\partial R_1^2} - \frac{1}{2m_2}\frac{\partial^2}{\partial R_2^2} - M^+[(j+a)(j+1+a) - \frac{1}{4}K^2]\right)\delta_{K,K'}\delta_{q,q'}\delta_{j,j'}.$$
 (14)

The rotational KEO also has a diagonal contribution as well as coupling *K* blocks differing by two:

$$\langle JKqj|T^{\text{rot}}|JK'q'j'\rangle = -(1+\delta_{0K})^{1/4} \frac{1}{2} M^{+} \left\langle j \left| \frac{c}{1-c^{2}} \right| j' \right\rangle$$

$$\times A_{JK'}^{\pm} \delta_{K,K'\pm 2} \delta_{q,q'} + (1+\delta_{0K})^{1/2}$$

$$\times \frac{1}{4} M^{-} \left\langle j \left| \frac{1}{(1-c^{2})^{1/2}} \right| j' \right\rangle$$

$$\times A_{JK'}^{\pm} \delta_{K,K'\pm 2} \delta_{q,1-q'}, \qquad (15)$$

where

$$A_{JK}^{\pm} = A_{J-K}^{\mp} = ([J(J+1) - K(K\pm 1)] \times [J(J+1) - K(K\pm 3) - 2])^{1/2}.$$
 (16)

Finally, the Coriolis KEO couples terms diagonal in K but differing in q,

$$\langle JKjq|T^{\text{cor}}|JK'j'q'\rangle = -\frac{1}{2}KM^{-}\left(\left\langle j\right| - \frac{c(1+2a+2j')}{(1-c^{2})^{1/2}} \left| j'\right\rangle + \left\langle j\left| \frac{2(j'+a)}{(1-c^{2})^{1/2}} \frac{(h_{j'-1}^{ab})^{1/2}}{(h_{j'}^{ab})^{1/2}} \right| j'-1\right\rangle\right)\delta_{KK'}\delta_{q,1-q'}.$$
(17)

Besides these terms, there is a special case that must be considered for the case when K=1. For this case there are extra terms both on the diagonal, augmenting $\langle JKqj|T^{\text{vib}}|JK'q'j\rangle$:

$$\langle JKqj|T_{K=1}^{\text{vib}}|JK'q'j\rangle$$

$$=\frac{(-1)^{1+q}}{4}J(J+1)M^{+}\left\langle j\left|\frac{c}{1-c^{2}}\right|j'\right\rangle\delta_{K,1}\delta_{K',1}\delta_{q,q'},$$
(18)

and on the off-diagonal augmenting $\langle JKjq|T^{\text{cor}}|JK'jq'\rangle$,

$$\langle JKqj|T_{K=1}^{\text{cor}}|JK'q'j\rangle = \frac{(-1)^{q'+s}}{4}J(J+1)M^{-}\langle j|(1-c^{2})^{-1/2}|j'\rangle \times \delta_{K,1}\delta_{K',1}\delta_{q,1-q'},$$
 (19)

where s is the parity of the radial basis; see Eq. (21).

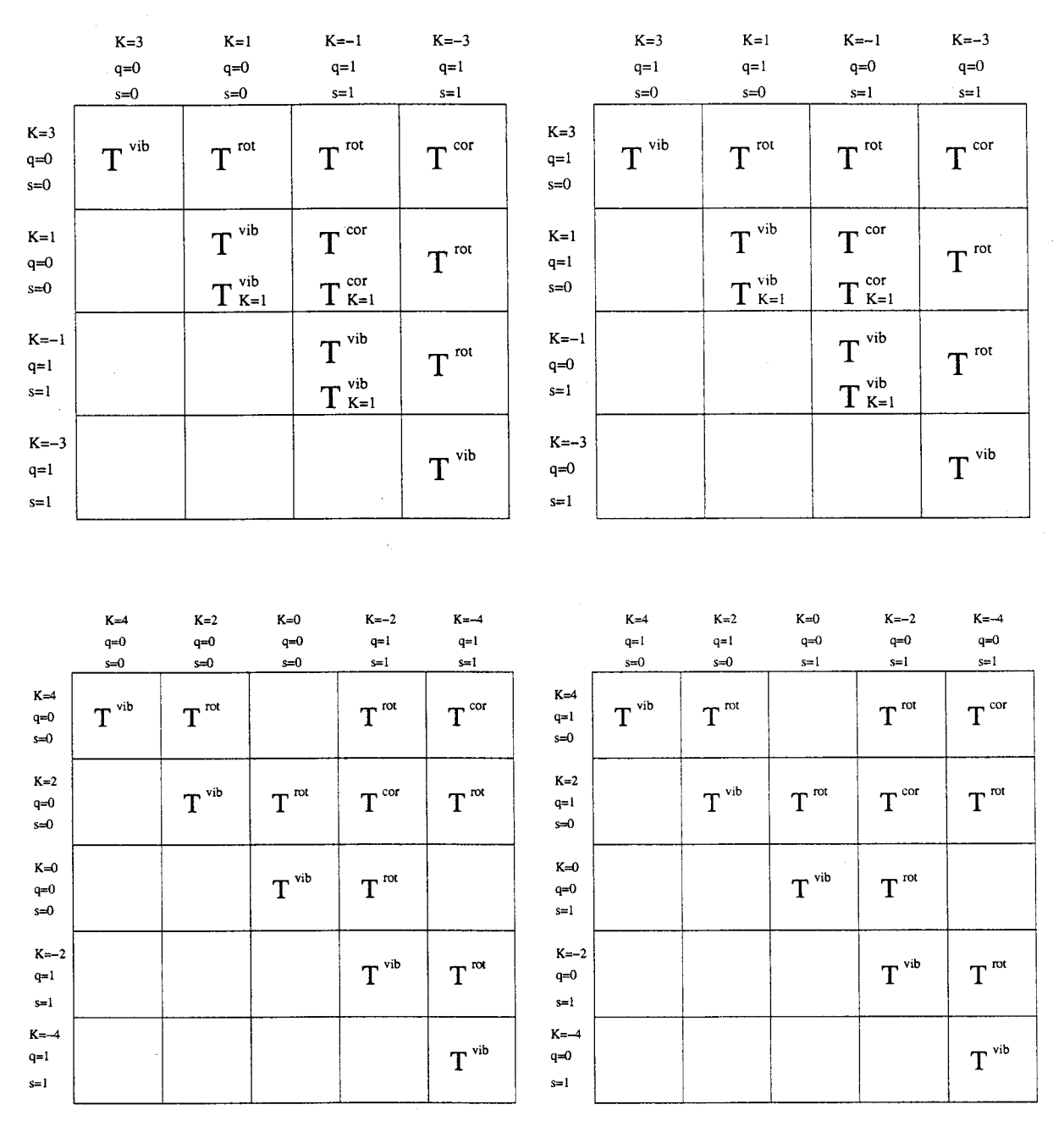


FIG. 1. Structure of the rotation-vibration matrix for the z-perpendicular embedding. The example is for the four symmetries of J=4. The matrices are real symmetric and only the upper triangle is given. Null blocks in the upper triangle are zero.

The above matrix elements include a cancellation between vibrational and rotational terms that is potentially singular at linear (i.e., θ =0 or π) geometries. If one follows Polyansky and Tennyson¹⁰ and use separate vibrational (m_v) and rotational (m_r) masses to model nonadiabatic effects, one final extra term is introduced. This term augments $T^{\rm vib}$,

$$\begin{split} \langle JKqj|T^{nBO}|JK'q'j\rangle \\ &= \left(1 - \frac{m_r}{m_v}\right) \frac{1}{4} [J(J+1) \\ &- K^2]M_r^+ \left\langle j \left| \frac{1}{1-c^2} \right| j' \right\rangle \delta_{KK'} \delta_{q,q'} \,, \end{split} \tag{20}$$

where the r subscript on the M^+ term signifies that the rotational mass is to be used.

III. METHOD OF SOLUTION

The z perpendicular embedding has been implemented within our DVR3D program suite²⁷ and will be part of a new addition to be published soon.³² These programs use a discrete variable representation (DVR) to represent the vibrational wave functions on a grid rather than as a basis function expansion. The DVR has the advantage that, within the so-called quadrature approximation, the potential is completely diagonal. Similarly diagonal in K matrix elements of the

form $\langle j|f(c)|j'\rangle$, where f(c) is some simple, nondifferential function of c, can also be evaluated straightforwardly in the DVR. Other bending matrix elements, such as those off-diagonal in K, are evaluated using the basis functions and then transformed to the DVR. ²⁶

Within a DVR, symmetrized radial functions can be written as

$$|\alpha,\beta,s\rangle = 2^{-1/2}(|\alpha,\beta\rangle + (-1)^s|\beta,\alpha\rangle), \quad \alpha > \beta, \quad s = 0,1,$$
(21)

$$|\alpha,\beta,s\rangle = |\alpha,\beta\rangle, \quad \alpha = \beta, \quad s = 0,$$

where α and β are grid points in the r_1 and r_2 coordinates, respectively. In this work, as elsewhere 26,27,31 we use Morse Oscillator-like functions to represent the motions in the radial coordinates.

For problems involving rotational excitation, we first solve the separate, pure "vibrational" problems defined by fixing a particular combination of K and q. Solutions of these problems are then used as a basis for the full rotation—vibration problem.³³ This two-step method has long been known to be a good method of treating problems with significant rotational excitation. It is particularly efficient when the intermediate quantum number, here K, is nearly conserved in the system in question. In favorable cases the computer time required to solve a given problem increases only linearly with J, instead of the J^3 scaling, which might be expected for direct approaches that do not first solve the intermediate problems.

IV. RESULTS

A. Water

Initially we tested our z-perpendicular method for the water molecule as we have considerable experience working on this molecule. In this case it is only necessary to consider rotationally excited states since calculations for J=0 are entirely equivalent to those performed by us routinely for this molecule using DVR3D; see Ref. 34, for example. There are two factors that come into play here: first for J=0 the Hamiltonian depends only on the vibrational coordinates used and not the axis embedding, and, second, in this case the Jacobi functions used here for the θ coordinate are the same as the Legendre polynomials used in our previous calculations.

Test calculations on $H_2^{16}O$ were performed using the barrier-corrected potential energy surface of Kain *et al.*³⁴ Calculations performed with our new program were compared with ones performed using Radau coordinates with a bisector embedding implemented as a standard option in DVR3D.²⁷ This embedding places the *z* axis in the plane of the molecule, perpendicular to the *x* axis, which bisects θ . Initial calculations used 21 radial grid points and 20 angular grid points. The two-dimensional radial Hamiltonians were diagonalized for each angular grid point. The lowest solutions of these problems were selected on energy grounds to provide a basis for the three-dimensional vibrational Hamil-

tonian. In each case a first step, vibrational Hamiltonian of size 2000 was diagonalized and 100 solutions retained from each K block to solve the full rotation-vibration problem, which thus gives a maximum secular matrix size of 100 $\times (J+1)$.

Table I compares for results of these calculations for J=3. For the lower lying levels there is excellent agreement between the two methods. However, for some higher states, particularly those with significant bending excitation, the agreement is less satisfactory. Calculations with the new method and 30 grid points in the θ coordinate show that the previous angular grid was not converged. Indeed, these new calculations still do not perform as well as the smaller bisector embedding calculations. We can therefore conclude that the z-perpendicular embedding is less suitable for water than the standard, bisector embedding.

That this new method is not optimal for water is not altogether surprising: a z-perpendicular embedding is not a natural one for water. It is well known that the K_a quantum number is the important one in the case of water. ³⁵ Part of the reason for the success of studies on water using the bisector embedding compared to other methods (see Ref. 36, for example) is because in this method k, the intermediate quantum number in the two-step variational procedure, is very close to K_a .

B. H₃⁺

The z-perpendicular embedding is not optimal for water, however, there are a number of reasons for suspecting it will be very good for H_3^+ . The most obvious of these is the observation that for a rigid symmetric top, projection of the J along the symmetry axis is a conserved quantum number. For H₃⁺ this axis is the one perpendicular to the plane of the molecular and, although vibrational angular momentum and Coriolis coupling complicate this picture, 21 K is still an important quantum number in this molecule. Less obviously, it transpires that the Radau coordinates used also have advantages since they are better able to deal with the singularities that arise when either vibrationally or rotationally excited H₃⁺ samples linear geometries. ¹⁷ This is because the barrier to linearity lies at finite values of r_1 and r_2 in Radau coordinates, whereas in Jacobi coordinates one of the (symmetry-related) barriers lies at $r_2 = 0$. This feature was actually the main reason we chose to explore this method.

An additional reason for using the *z*-perpendicular embedding concerns the model developed by Polyansky and Tennyson¹⁰ to represent rovibrational motion of the H₃⁺ *ab initio*. This model yielded results of approaching spectroscopic accuracy partly by using different masses for the vibrational and rotational motions of the molecule, which leads to the extra term discussed above; see Eq. (20). However, any treatment that distinguishes between vibrational and rotational motion depends implicitly on the body-fixed axis system employed. Many years ago, Eckart³⁷ demonstrated how to define axes that lead to optimal separation of vibrational and rotational motion. Recently some progress has been made in marrying Eckart's embedding with internal

TABLE I. Energy levels, in cm⁻¹, for water with J=3. Old refers to calculations performed with program DVR3D (Ref. 27) and the bisector embedding. New1 used the z-perpendicular embedding and the same size basis. New2 uses an increased angular grid.

JK_aK_c	$v_{1}v_{2}v_{3}$	Old	New1	New2	Old- New1	Old- New2
303	000	136.778	136.777	136.772	0.001	0.00
322	000	206.271	206.271	206.267	0.000	0.004
321	000	212.136	212.136	212.132	0.001	0.00
303	010	1734.360	1734.364	1734.363	-0.004	-0.00
322	010	1816.187	1816.188	1816.186	0.000	0.00
321	010	1821.744	1821.745	1821.743	-0.001	0.00
303	020	3293.977	3293.969	3293.943	0.008	0.03
322	020	3392.290	3392.301	3392.284	-0.012	0.00
321	020	3397.368	3397.385	3397.361	-0.012	0.00
303	100	3794.894	3794.893	3794.888	0.001	0.00
322	100	3862.352	3862.352	3862.348	0.000	0.00
321	100	3868.250	3868.249	3868.245	0.001	0.00
313	001	3898.137	3898.137	3898.135	0.000	0.00
312	001	3929.429	3929.429	3929.427	0.000	0.00
331	001	4032.508	4032.508	4032.507	0.000	0.00
330	001	4032.745	4032.746	4032.744	0.000	0.00
303	030	4811.576	4812.134	4811.895	-0.558	-0.31
322	030	4933.621	4933.796	4933.646	-0.176	-0.02
321	030	4938.029	4938.298	4938.074	-0.269	-0.04
303	110	5375.760	5375.768	5375.764	-0.009	-0.00
322	110	5455.036	5455.039	5455.035	-0.003	0.00
321	110	5460.606	5460.611	5460.605	-0.005	0.00
313	011	5478.103	5478.103	5478.103	0.003	0.00
313	011	5511.276	5511.277	5511.276	-0.000	0.00
331	011	5634.765	5634.765	5634.765	0.001	0.00
330	011	5634.965	5634.965	5634.965	0.000	0.00
303	040	6282.723	6285.366	6282.664	-2.643	0.06
322	040	6439.429				-0.21
321	040	6443.019	6441.140 6445.405	6439.640 6443.323	-1.711 -2.386	-0.21
303	120				-2.380 -0.066	0.01
322	120	6918.595 7013.572	6918.661 7013.622	6918.579 7013.571	-0.066 -0.050	0.00
322	120		7013.022	7013.371	-0.030 -0.071	-0.00
313		7018.408				
	021	7024.118	7024.125	7024.110 7058.825	-0.007	0.00
312	021	7058.832	7058.839		-0.007	0.00
331 330	021	7208.961	7208.965	7208.960	-0.004	0.00
	021	7209.121	7209.126	7209.120	-0.005	0.00
303	200	7340.016	7340.018	7340.015	-0.001	0.00
322	200	7391.915	7391.915	7391.912	0.000	0.00
321	200	7404.809	7404.809	7404.807	0.000	0.00
313	101	7411.649	7411.649	7411.647	-0.001	0.00
312	101	7423.739	7423.739	7423.737	0.000	0.00
331	101	7523.051	7523.051	7523.049	0.000	0.00
330	101	7523.298	7523.299	7523.296	0.000	0.00
303	002	7583.353	7583.353	7583.352	0.000	0.00
322	002	7645.721	7645.721	7645.720	0.000	0.00
321	002	7652.426	7652.426	7652.425	0.000	0.00
303	130	8419.893	8421.274	8420.600	-1.381	-0.70
322	130	8532.728	8532.837	8532.810	-0.108	-0.08
321	130	8537.722	8538.204	8537.806	-0.482	-0.08
313	031	8542.503	8543.182	8542.649	-0.679	-0.14
312	031	8569.740	8570.004	8569.837	-0.264	-0.09
331	031	8755.948	8755.985	8755.955	-0.036	-0.00
330	031	8756.069	8756.107	8756.076	-0.039	-0.00
303	210	8903.035	8903.079	8903.064	-0.044	-0.02
322	210	8953.804	8953.809	8953.807	-0.005	-0.00
321	210	8978.638	8978.646	8978.640	-0.008	-0.00

coordinates, 38 although the resulting Hamiltonians are complicated. For triatomic molecules, such as H_3^+ , all embedding, including Eckart's automatically place one axis perpendicular to the plane of the molecule. Since the size of the

centrifugal coupling term depends on the difference between rotational constants, it is advantageous to choose the z axis so that its rotational constant is the most distinct. For H_3^+ this is clearly perpendicular to the molecular plane since, at least

TABLE II. Energy levels, in cm⁻¹, for H_3^+ with J=3.

		PT	DPT	Obs.		Obs
Rot.	Vib.	(Ref. 10)	(Ref. 41)	(Ref. 42)	Calc.	Calc.
(3,3)	000	315.3353	315.351	315.35	315.349	0.001
(3,2)	00_{0}	428.0315	428.024	428.019	427.999	0.020
(3,1)	00_{0}	494.7973	494.771	494.777	494.732	0.045
(3,4)	01^{1}	516.9207	516.885	516.873	516.842	0.031
(3,4)	01^{1}	2719.4145	2719.488	2719.483	2719.414	0.069
(3,3)	01^{1}	2876.8132	2876.848	2876.845	2876.754	0.091
(3,2)l	01^{1}	2931.3321	2931.380	2931.365	2931.316	0.049
(3,2)u	01^{1}	2992.4228	2992.443	2992.433	2992.344	0.089
(3,1)l	01^{1}	3002.8901	3002.909	3002.904	3002.819	0.085
(3,0)	01^{1}	3025.9618	3025.965	3025.948	3025.867	0.081
(3,1)u	01^{1}	3063.4774	3063.481	3063.476	3063.381	0.095
(3,3)	10^{0}	3485.3835	3485.308	3485.306	3485.373	-0.067
(3,2)	10^{0}	3595.8505	3595.744	3595.74	3595.785	-0.045
(3,1)	10^{0}	3661.2187	3661.090	3661.081	3661.116	-0.035
(3,0)	10^{0}	3682.8684	3682.730	3682.751	3682.751	0.000
(3,3)	02^{0}	5078.9349	5078.933	5078.93	5078.911	0.019
(3,5)	02^{2}	5105.2679	5105.284	5105.293	5105.244	0.049
(3,2)	02^{0}	5210.8302	5210.794	5210.796	5210.746	0.050
(3,1)	02^{0}	5282.3792	5282.315	5282.318	5282.257	0.061
(3,4)	02^{2}	5299.2553	5299.233	5299.227	5299.173	0.054
(3,0)	02^{0}	5305.6346	5305.583	5305.582	5305.52	0.062
(3,3)	02^{2}	5431.1736	5431.118	5431.121	5431.055	0.066
(3,1)l	02^{2}	5486.4840	5486.458	5486.456	5486.451	0.005
(3,2)	02^{2}	5533.7950	5533.738	5533.729	5533.668	0.061
(3,0)	02^{2}	5567.4027	5567.403	5567.387	5567.357	0.030
(3,1)u	02^{2}	5573.8250	5573.767	5573.763	5573.707	0.056
(3,4)	11^{1}	5764.7880	5764.873	5764.879	5764.757	0.122
(3,3)	11^1	5910.0479	5910.105	5910.108	5909.960	0.148
(3,2)l	11^{1}	5949.3658	5949.454	5949.444	5949.326	0.118
(3,2)u	11^{1}	6015.9046	6015.945	6015.947	6015.794	0.153
(3,1)l	11^{1}	6023.7099	6023.772	6023.757	6023.612	0.145
(3,0)	11^{1}	6047.4949	6047.543	6047.565	6047.371	0.194
(3,1)u	11^1	6080.9447	6080.969	6080.967	6080.82	0.147
(3,2)l	03^{1}	7362.2861	7362.213	7362.203	7362.247	-0.044
(3,6)	03^{3}	7418.4465	7418.485	7418.433	7418.405	0.028
(3,4)	03^{3}	7796.5703	7796.715	7796.716	7796.432	0.284
(3,3)	03^{3}	7854.3313	7854.569	7854.413	7854.188	0.225
(3,0)	03^{3}	7866.1204	7866.782	7866.298	7866.077	0.221
(3,2)	03^{3}	8017.8451	8017.963	8017.719	8017.708	0.011
(3,3)	12^{0}	8138.8933	8139.345	8139.068	8138.839	0.229
(3,3)	12^{2}	8301.5470	8302.413	8302.106	8301.408	0.698
(3,0)	12^{2}	8424.8200	8425.805	8425.419	8424.708	0.711

for geometries with D_{3h} symmetry, all orientiations of the axes in the plane of the molecular are equivalent. This suggests that the z-perpendicular embedding employed here may be near optimal for separation of vibrational and rotational motion, and hence offer the possibility of further improvements on the Polyansky–Tennyson method.

Calculations were performed for $\mathrm{H_3^+}$ for $J\!=\!0$ to 15 inclusive. These calculations mirror those of Polyansky and Tennyson, who used Born–Oppenheimer potentials, including an electronic relativistic correction, and adiabatic surfaces derived from the ultrahigh accuracy electronic structure calculations of Cencek *et al.* Our calculations used 21 point grids for the Morse oscillatorlike functions that were defined using the parameters $r_e\!=\!1.8~a_0$, $D_e\!=\!0.07~E_h$, and $\omega_e\!=\!0.0118~\mathrm{a.u.}$, which we optimized for the problem. Here 40-points were used in the angular grid and the first step Hamiltonian of size 2500, after diagonalization and

trunction the 40 stretch-only problems, was diagonalized to provide 200 functions for each K,q combination for the full Hamiltonian. This level of calculation converges the results quoted here to within 0.005 cm⁻¹ in all cases.

A full set of results are given in the EPAPS archive³⁹ and only sample results for J=3 and J=10 are presented here. Before analyzing these in detail, it is worth noting that previous high accuracy work using Jacobi coordinates and inplane embedding of the z axis could not give reliable results for J=10 because of difficulties with treating linear geometries.⁴⁰

Tables II and III compare our results with the newly derived H_3^+ experimental energy levels of Lindsay and McCall, 42 which supercede those of Dinelli *et al.* 40 The quantum number notation used also follows Lindsay and McCall. Table II also quotes the *ab initio* results of Polyansky and Tennyson $(\mathrm{PT})^{10}$ and the earlier results of Dinelli,

TABLE III. Energy levels, in cm⁻¹, for H_3^+ with J = 10.

Rot.	Vib.	Obs. ⁴²	Calc.	ObsCalc.
(10,9)	000	2856.725	2856.684	0.041
(10,8)	00^{0}	3196.907	3196.794	0.113
(10,7)	00^{0}	3484.761	3484.644	0.117
(10,6)	00^{0}	3726.566	3726.357	0.209
(10,5)	00^{0}	3926.180	3925.925	0.255
(10,4)	00^{0}	4086.425	4086.148	0.277
(10,3)	00^{0}	4215.251	4214.933	0.318
(10,1)	00^{0}	4348.434	4348.025	0.409
(10,11)	01^{1}	4539.256	4539.238	0.018
(10,9)l	01^{1}	5198.220	5198.239	-0.019
(10,9)u	01^{1}	5454.430	5454.270	0.160
(10,8)l	01^{1}	5555.440	5555.357	0.083
(10,8)u	01^{1}	5827.721	5827.558	0.163
(10,7)l	01^{1}	5842.715	5842.560	0.155
(10,6)l	01^{1}	6087.522	6087.310	0.212
(10,7)u	01^{1}	6145.225	6145.005	0.220
(10,5)l	01^{1}	6226.722	6226.533	0.189
(10,4)l	01^{1}	6401.106	6400.830	0.276
(10,6)u	01^{1}	6412.314	6412.050	0.264
(10,3)l	01^{1}	6539.949	6539.591	0.358
(10,5)u	01^{1}	6628.648	6628.351	0.297
(10,12)	02^{2}	6668.953	6669.077	-0.124
(10,4)u	01^{1}	6811.749	6811.431	0.318
(10,3)u	01^{1}	6959.028	6958.697	0.331
(10,5)	10^{0}	6967.296	6966.989	0.307
(10,10)	02^{0}	7035.014	7035.222	-0.208
(10,1)u	01^{1}	7055.343	7054.927	0.416
(10,0)	01^{1}	7080.430	7080.051	0.379
(10,11)	02^{2}	7219.741	7219.692	0.049
(10,8)l	02^{2}	8006.247	8006.266	-0.019
(10,7)	02^{0}	8110.218	8109.502	0.716
(10,8)	11^{1}	8380.427	8380.135	0.292
(10,6)u	11^{1}	9346.885	9346.458	0.427
(10,12)	12^{2}	9593.440	9590.598	2.842

Polyansky, and Tennyson (DPT),⁴¹ who used spectroscopic data to refine their potentials. Both calculations explicitly included allowance for non-Born-Oppenheimer effects.

As with the previous study by PT, the level of agreement with experiment for a pure *ab initio* treatment is generally excellent. For J=3, for which a direct comparison with PT can be made, the new results are somewhat better in two respects. Except for the highest vibrational states, discussed below, the overall deviation from experiment is smaller. Furthermore, it is smoother, with errors of similar sign and magnitude (typically 0.05 cm⁻¹) for J=3 levels belonging to a particular vibrational state.

The present calculation is the first time states with J > 5 have been computed using the PT model for vibrational nonadiabatic effects. Looking at the J = 10 results presented in Table III, it is apparant that the error in the individual levels is systematically larger (typically $0.2 \, \mathrm{cm}^{-1}$) than those observed for J = 3. It should be noted that the PT model uses nuclear masses for the rotational KEO¹⁰ and makes no other allowance for rotational non-adiabatic effects. It would seem that the deviations from experiment, which we find increase systematically with J, are due to the neglect of these rotational nonadiabatic effects. We are presently working on this aspect of the problem.

Finally, as noted above there are larger deviations from

experiment for levels associated with the highest vibrational states. This is true for both J=3 and J=10 calculations. Tests comparing results obtained using both PTs and the Jacquet et al. 7 fits to the Cencek et al. ab initio data 6 show that, unlike the lower states, these vibrational states show considerable sensitivity to the exact fit of the ab initio points, which gives the potential in an analytic form. Both these fits reproduce the Cencek et al. ab initio data to high accuracy so it would seem that this sensitivity is to regions of the surface not covered in this ab initio study. Comparisons with more comprehensive but slightly less accurate ab initio calculations⁴³ confirmed that there are significant, asymmetric low-lying regions of the potential that were not covered by the 69 MBB⁴⁴ grid point used in the Cencek et al. calculations. It is the different extrapolations into regions not covered by these points that account for the different results obtained.

V. CONCLUSION

Triatomic rotation–vibration Hamiltonians that place the *z* axis of the body-fixed axis system perpendicular to the plane of the molecule have been derived independently by Sutcliffe and co-workers^{23,24} and Sarkur *et al.*²⁵ We have implemented a two-step procedure based on these Hamiltonians using a discrete variable representation (DVR) for the vibrational coordinates and solutions of Coriolis decoupled rotational problems as a basis for the full rotation–vibration problem. These programs have been included as part of our updated DVR3D program suite and will be published soon.³²

Test calculations using our new procedure for water show that this method is not as efficient for this molecule as one that places the z axis close to the A rotation axis of the system. Conversely, calculations on H_3^+ suggest that this method has a number of advantages for this system, which means that it is appropriate for treating both states with high vibrational or high rotational excitation, or indeed both, suggesting that the method should be suitable for treating rotationally excited states at dissociation.

A comparison with high accuracy calculations, performed beyond the Born–Oppenheimer approximation, with experimentally derived energy levels shows good agreement for levels with low rotational excitation. This is in line with a recent study on the overtone spectra of H_2D^+ and D_2H^+ found that the use of an effective vibrational mass gave excellent predictions for new low-temperature experiments on these species. However, our calculations do display systematic disagreement with increasing rotational excitation. Since the method used to treat nonadiabatic coupling in these calculations only allows for vibrational effects, it is probable that these errors are due to rotationally nonadiabatic effects. We are currently working on this aspect of the problem.

ACKNOWLEDGMENTS

The authors thank Tucker Carrington and Brian Sutcliffe for helpful discussions on their Hamiltonians. This work was supported by the UK Engineering and Physical Science Research Council. The work of O.I.P. was supported in part by the Russian Fund for Fundamental Studies.

APPENDIX: DERIVATION OF THE MATRIX ELEMENTS

In this appendix we derive the angular matrix elements given in Eqs. (15)–(19) for the kinetic energy operators (KEOs) (2)–(4) using the angular basis functions (11) and rotational functions (13). A less full account of this derivation can be found in Sarkar *et al.*²⁵ Each KEO is considered in turn.

1. Vibrational operator, Tvib

This operator is diagonal in both K and q,

$$\begin{split} \langle JKqj|T^{\text{vib}}|JKqj'\rangle &= \left(-\frac{1}{2m_1}\frac{\partial^2}{\partial R_1^2} - \frac{1}{2m_2}\frac{\partial^2}{\partial R_2^2}\right)\delta_{jj'} \\ &+ \langle j| - M^+ \frac{\partial}{\partial c}(1-c^2)\frac{\partial}{\partial c} \\ &+ \frac{1}{4}(G_{xx} + G_{yy})(J(J+1) \\ &- K^2)|j'\rangle + \frac{1}{4}K^2M^+\delta_{jj'} \,. \end{split} \tag{A1}$$

Following Johnson,⁴⁶ the matrix element over the angular integral can be evaluated as follows:

$$\left\langle j \middle| -\frac{\partial}{\partial c} (1 - c^2) \frac{\partial}{\partial c} + \frac{1}{4} [J(J+1) - K^2] \right.$$

$$\left. \times \left(\frac{1}{1+c} + \frac{1}{1-c} \right) \middle| j' \right\rangle$$

$$= -\left\langle j \middle| \frac{\partial}{\partial c} (1 - c^2) \frac{\partial}{\partial c} - \frac{1}{2} a^2 \frac{1}{1-c} - \frac{1}{2} b^2 \frac{1}{1+c} \middle| j' \right\rangle$$

$$= -\left(j + \frac{a+b}{2} \right) \left(j + 1 + \frac{a+b}{2} \right) \delta_{jj'}, \tag{A2}$$

where, for the present study, a and b are defined by Eq. (12) and hence give the J dependence of these matrix elements.

2. The rotational operator T^{rot}

Within the *z*-perpendicular embedding, the rotational KEO is given by

$$T^{\text{rot}} = \frac{1}{2} \left[G_{xx} J_x^2 + G_{yy} J_y^2 + G_{zz} J_z^2 + G_{xy} (J_x J_y + J_y J_x) \right].$$
(A3)

Letting this act on a rotation matrix, $|JK\rangle$, gives

$$\langle JK|T^{\text{rot}}|JK'\rangle = \frac{1}{8} [(G_{xx} - G_{yy} \pm 2\iota G_{xy})A_{JK}^{\pm} \delta_{K,K'\pm 2} + [2(G_{xx} + G_{yy})(J(J+1) - K^2) + 4K^2 G_{zz}]\delta_{K,K'}, \tag{A4}$$

where A_{JK}^{\pm} is defined by Eq. (16). Using the symmetrized rotational functions gives

$$\langle JKq|T^{\text{rot}}|J'K'q'\rangle = \frac{(1+\delta_{0,K})^{1/2}(1+\delta_{0,K'})^{1/2}}{2\iota^{q+q'}}(\langle JK|T^{\text{rot}}|J'K'\rangle + (-1)^{q+K}\langle J, -K|T^{\text{rot}}|J'K'\rangle + (-1)^{q'+K'}\langle JK|T^{\text{rot}}|J', -K'\rangle + (-1)^{q+K+q'+K'}\langle J, -K|T^{\text{rot}}|J', -K'\rangle), \tag{A5}$$

$$\begin{split} &= \frac{1}{16} \frac{1}{\iota^{q+q'}} ((1+\delta_{0,K})^{1/2} (1+\delta_{0,K'})^{1/2} (G_{xx} - G_{yy} \pm 2 \iota G_{xy}) A_{JK'}^{\pm} \delta_{K,K'\pm 2} \\ &\quad + (2(G_{xx} + G_{yy}) (J(J+1) - K^2) + 4K^2 G_{zz}) \delta_{K,K'} + (-1)^{q+q'} [(1+\delta_{0,K})^{1/2} (1+\delta_{0,K'})^{1/2} \\ &\quad \times (G_{xx} - G_{yy} \pm 2 \iota G_{xy}) A_{J-K'}^{\pm} \delta_{-K,-K'\pm 2} + [2(G_{xx} + G_{yy}) (J(J+1) - K^2] + 4K^2 G_{zz}) \delta_{K,K'}] \}, \ \, \text{(A6)} \end{split}$$

$$= \frac{1}{16} \frac{1}{\iota^{q+q'}} \left[\delta_{K,K'\pm 2} (1+\delta_{0,K})^{1/2} (1+\delta_{0,K'})^{1/2} \left[A_{JK'}^{\pm} (G_{xx} - G_{yy} \pm 2\iota G_{xy}) + (-1)^{q+q'} A_{JK'}^{\pm} (G_{xx} - G_{yy} \pm 2\iota G_{xy}) \right] \right]$$

$$= \frac{1}{16} \frac{1}{\iota^{q+q'}} \left[\delta_{K,K'\pm 2} (1+\delta_{0,K})^{1/2} \left[A_{JK'}^{\pm} (G_{xx} - G_{yy} \pm 2\iota G_{xy}) + (-1)^{q+q'} A_{JK'}^{\pm} (G_{xx} - G_{yy} \pm 2\iota G_{xy}) \right] \right]$$

$$= \frac{1}{16} \frac{1}{\iota^{q+q'}} \left[\delta_{K,K'\pm 2} (1+\delta_{0,K})^{1/2} \left[A_{JK'}^{\pm} (G_{xx} - G_{yy} \pm 2\iota G_{xy}) + (-1)^{q+q'} A_{JK'}^{\pm} (G_{xx} - G_{yy} \pm 2\iota G_{xy}) \right] \right]$$

$$= \frac{1}{16} \frac{1}{\iota^{q+q'}} \left[\delta_{K,K'\pm 2} (1+\delta_{0,K})^{1/2} \left[A_{JK'}^{\pm} (G_{xx} - G_{yy} \pm 2\iota G_{xy}) + (-1)^{q+q'} A_{JK'}^{\pm} (G_{xx} - G_{yy} \pm 2\iota G_{xy}) \right] \right]$$

$$= \frac{1}{16} \frac{1}{\iota^{q+q'}} \left[\delta_{K,K'\pm 2} (1+\delta_{0,K})^{1/2} \left[A_{JK'}^{\pm} (G_{xx} - G_{yy} \pm 2\iota G_{xy}) + (-1)^{q+q'} A_{JK'}^{\pm} (G_{xx} - G_{yy} \pm 2\iota G_{xy}) \right] \right]$$

$$= \frac{1}{16} \frac{1}{\iota^{q+q'}} \left[\delta_{K,K'\pm 2} (1+\delta_{0,K})^{1/2} \left[A_{JK'}^{\pm} (G_{xx} - G_{yy} \pm 2\iota G_{xy}) + (-1)^{q+q'} A_{JK'}^{\pm} (G_{xx} - G_{yy} \pm 2\iota G_{xy}) \right]$$

$$= \frac{1}{16} \frac{1}{\iota^{q+q'}} \left[\delta_{K,K'\pm 2} (1+\delta_{0,K})^{1/2} \left[A_{JK'}^{\pm} (G_{xx} - G_{yy} \pm 2\iota G_{xy}) + (-1)^{q+q'} A_{JK'}^{\pm} (G_{xx} - G_{yy} \pm 2\iota G_{xy}) \right]$$

$$= \frac{1}{16} \frac{1}{\iota^{q+q'}} \left[\delta_{K,K'\pm 2} (1+\delta_{0,K})^{1/2} \left[A_{JK'\pm 2} (1+\delta_{0$$

$$= (\frac{1}{8}(1 + \delta_{0,K})^{1/2}(1 + \delta_{0,K'})^{1/2}(G_{xx} - G_{yy})A_{JK'}^{\pm}, \delta_{K,K'\pm 2} + [\frac{1}{4}(G_{xx} + G_{yy})(J(J+1) - K^{2}) + \frac{1}{2}K^{2}G_{zz}]\delta_{K,K'})\delta_{q,q'}^{\pm} \pm \frac{1}{4}G_{xy}A_{JK'}^{\pm}, \delta_{K,K'\pm 2}\delta_{q,1-q'}.$$
(A8)

3. Coriolis term in the rotational basis

The Coriolis term couples rotational basis functions that differ in q but have the same value of K:

$$\langle JKq|T^{\text{cor}}|J'K'q'\rangle$$

$$= \frac{1}{2\iota^{q+q'}} [\langle JK|T^{\text{cor}}|J'K'\rangle$$

$$+ (-1)^{q+K}\langle J, -K|T^{\text{cor}}|J'K'\rangle$$

$$+ (-1)^{q'+K'}\langle JK|T^{\text{cor}}|J', -K'\rangle$$

$$+ (-1)^{q+K+q'+K'}\langle J, -K|T^{\text{cor}}|J', -K'\rangle], \quad (A9)$$

$$T^{\text{cor}}|J\pm K\rangle = \mp \frac{\iota}{2}FK|J\pm K\rangle,$$
 (A10)

where the Coriolis coupling is provided by

$$F = \frac{\partial}{\partial c} G_{cz} + G_{cz} \frac{\partial}{\partial c}.$$
 (A11)

Using the symmetry of the rotational functions gives

$$\langle JKq|T^{\rm cor}|J'K'q'\rangle$$

$$= \frac{1}{4\iota^{q+q'-1}} FK[-1+(-1)^{q+q'}] \delta_{KK'} (1-\delta_{K0}), \tag{A12}$$

which can be simplified to

$$\langle JKq|T^{\text{cor}}|J'K'q'\rangle = -\frac{1}{2}FK\delta_{KK'}(1-\delta_{K0})\delta_{q,1-q'}.$$
(A13)

In the bending basis, the matrix elements for operator F are

$$\begin{split} \left\langle j \middle| -\frac{1}{2} M^{-} \left(\frac{\partial}{\partial c} (1 - c^{2})^{1/2} + (1 - c^{2})^{1/2} \frac{\partial}{\partial c} \right) \middle| j' \right\rangle \\ &= -\frac{1}{2} M^{-} \left\langle j \middle| -\frac{c}{(1 - c^{2})^{1/2}} + 2(1 - c^{2})^{1/2} \frac{\partial}{\partial c} \middle| j' \right\rangle \\ &= -\frac{1}{2} M^{-} \left(\left\langle j \middle| -\frac{c(1 + 2a + 2j)}{(1 - c^{2})^{1/2}} \middle| j' \right\rangle \\ &+ \left\langle j \middle| \frac{2(j + a)}{(1 - c^{2})^{1/2}} \frac{(h_{j-1}^{ab})^{1/2}}{(h_{j}^{ab})^{1/2}} \middle| j' - 1 \right\rangle \right). \end{split}$$
(A14)

4. Extra terms for the K=1 case

Part of the rotational KEO T^{rot} , referred to as $T_{(2)}^{\text{rot}}$ below, couples rotational functions that differ in K by two. A special case arises for symmetrized basis functions with K=1 as this operator couples rotation matrices $|J1\rangle$ with $|J-1\rangle$, even for the diagonal element. A similar situation is found for the "bisector embedding case" which differs from the present Hamiltonian in that y and z axis embeddings are swapped over.²⁶

The extra contribution to the diagonal (in K) block of the matrix that arises from this coupling of the K=1 basis functions is

$$\langle JKq|T^{\text{rot}}|J'K'q'\rangle$$

$$= \frac{1}{2} (\langle JK|T^{\text{rot}}|J'K'\rangle + (-1)^{q+K}\langle J-K|T^{\text{rot}}|J'K'\rangle$$

$$+ (-1)^{q'+K'}\langle JK|T^{\text{rot}}|J'-K'\rangle$$

$$+ (-1)^{q+K+q'+K'}\langle J-K|T^{\text{rot}}|J'-K'\rangle) \times P, \quad (A15)$$

where P is a phase factor defined by

$$P = \frac{1}{\iota^{q+q'}} = 1, \qquad q' = q = 0$$

$$= -1, \quad q' = q = 1$$

$$= -i, \quad q' \neq q.$$
(16)

For the truly diagonal, i.e., q = q', case the extra term is

$$\frac{P}{2} \big[\big\langle J1 \big| T_{(2)}^{\rm rot} \big| J - 1 \big\rangle + (-1)^{q'-1} \big\langle J1 \big| T_{(2)}^{\rm rot} \big| J1 \big\rangle + (-1)^{q+1}$$

$$\times \langle J - 1 | T_{(2)}^{\text{rot}} | J - 1 \rangle + (-1)^{q'+q} \langle J - 1 | T_{(2)}^{\text{rot}} | J 1 \rangle],$$
 (A17)

substituting in

$$\langle JK|T_{(2)}^{\text{rot}}|JK'\rangle = \frac{1}{8}[(G_{xx} - G_{yy} \pm 2\iota G_{xy})A_{JK'}^{\pm}\delta_{K,K'\pm 2},$$
(A18)

gives the final extra contribution to the q=q' K=1 diagonal block as

$$\langle J1q|T^{K=1}|J1q\rangle = \frac{1}{8}P\,\delta_{qq'}(G_{xx} - G_{yy})A_{J1}^{+}$$

= $\frac{(-1)^{q+1}}{4}J(J+1)\frac{c}{1-c^{2}}M^{+}.$ (A19)

For the off-diagonal case, i.e., $q \neq q'$, the extra contribution is

$$\begin{split} \langle J1q|T^{K=1}|J1q'\rangle \\ &= \frac{1}{2} [\langle J1|T^{\text{rot}}_{(2)}|J1\rangle + (-1)^{q'+1}\langle J1|T^{\text{rot}}_{(2)}|J-1\rangle \\ &+ (-1)^{q+1}\langle J-1|T^{\text{rot}}_{(2)}|J1\rangle \\ &+ (-1)^{q'+q}\langle J-1|T^{\text{rot}}_{(2)}|J-1\rangle] \\ &= \frac{(-1)^{q'+1}}{4} J(J+1) \frac{1}{(1-c^2)^{1/2}} M^- \delta_{q,1-q'} \,. \end{split} \tag{A21}$$

¹T. R. Geballe, Philos. Trans. R. Soc. London, Ser. A 358, 2503 (2000).

²J. Tennyson and S. Miller, Spectrochim. Acta, Part A 57, 661 (2001).

³T. Oka, Rev. Mod. Phys. **64**, 1141 (1992).

⁴I. R. McNab, Adv. Chem. Phys. **89**, 1 (1994).

⁵ J. Tennyson, Rep. Prog. Phys. **58**, 421 (1995).

⁶W. Cencek, J. Rychlewski, R. Jaquet, and W. Kutzelnigg, J. Chem. Phys. 108, 2831 (1998)

⁷R. Jaquet, W. Cencek, W. Kutzelnigg, and J. Rychlewski, J. Chem. Phys. **108**, 2837 (1998).

⁸B. M. Dinelli, C. R. Le Sueur, J. Tennyson, and R. D. Amos, Chem. Phys. Lett. **232**, 295 (1995).

⁹O. L. Polyansky, B. M. Dinelli, C. R. Le Sueur, and J. Tennyson, J. Chem. Phys. **102**, 9322 (1995).

¹⁰O. L. Polyansky and J. Tennyson, J. Chem. Phys. **110**, 5056 (1999).

¹¹B. J. McCall, Phil. Trans. R. Soc. London, Ser. A 358, 2385 (2000) and Ph.D. thesis, University of Chicago, 2001.

¹² J. R. Henderson and J. Tennyson, Chem. Phys. Lett. **173**, 133 (1990).

¹³ J. R. Henderson, J. Tennyson, and B. T. Sutcliffe, J. Chem. Phys. **98**, 7191 (1993)

¹⁴M. J. Bramley, J. W. Tromp, T. Carrington, Jr., and G. C. Corey, J. Chem. Phys. **100**, 6175 (1994).

- ¹⁵ J. R. Henderson and J. Tennyson, Mol. Phys. **89**, 953 (1996).
- ¹⁶ V. A. Mandelshtam and H. S. Taylor, J. Chem. Soc., Faraday Trans. 93, 847 (1997).
- ¹⁷ J. Tennyson, M. A. Kostin, H. Y. Mussa, O. L. Polyansky, and R. Prosmiti, Philos. Trans. R. Soc. London, Ser. A 358, 2419 (2000).
- ¹⁸J. K. G. Watson, Can. J. Phys. **72**, 238 (1994).
- ¹⁹L. Wolniewicz and J. Hinze, J. Chem. Phys. **101**, 9817 (1994).
- ²⁰ H. Wei and T. Carrington, Jr., J. Chem. Phys. **101**, 1343 (1994).
- ²¹ J. K. G. Watson, J. Mol. spectrosc. **103**, 350 (1984).
- ²² J. Tennyson, J. Chem. Phys. **98**, 9658 (1993).
- ²³ J. R. Henderson, J. Tennyson, and B. T. Sutcliffe, Philos. Mag. B 69, 1027 (1994)
- ²⁴N. Anderson and B. T. Sutcliffe, Int. J. Quantum Chem. **60**, 37 (1996).
- ²⁵ P. Sarkar, N. Poulin, and T. Carrington, Jr., J. Chem. Phys. **110**, 10269 (1999).
- ²⁶ J. Tennyson and B. T. Sutcliffe, Int. J. Quantum Chem. **42**, 941 (1992).
- ²⁷ J. Tennyson, J. R. Henderson, and N. G. Fulton, Comput. Phys. Commun. 86, 175 (1995).
- ²⁸B. R. Johnson and W. P. Reinhardt, J. Chem. Phys. **85**, 4538 (1986).
- ²⁹D. Huber, Int. J. Quantum Chem. **28**, 245 (1985).
- ³⁰ D. M. Brink and G. R. Satchler, *Angular Momentum*, 2nd ed. (Clarendon, Oxford, 1968).
- ³¹ J. Tennyson and B. T. Sutcliffe, J. Chem. Phys. **77**, 4061 (1982).
- ³² J. Tennyson, M. A. Kostin, G. J. Harris, P. Barletta, O. L. Polyansky, and N. F. Zobov (unpublished).

- ³³ J. Tennyson and B. T. Sutcliffe, Mol. Phys. **58**, 1067 (1986).
- ³⁴ J. S. Kain, O. L. Polyansky, and J. Tennyson, Chem. Phys. Lett. **317**, 365 (2000).
- ³⁵O. L. Polyansky, J. Mol. Spectrosc. **112**, 79 (1985).
- ³⁶O. L. Polyansky, N. F. Zobov, S. Viti, J. Tennyson, P. F. Bernath, and L. Wallace, J. Mol. Spectrosc. 186, 422 (1997).
- ³⁷C. Eckart, Phys. Rev. **47**, 552 (1935).
- ³⁸H. Wei and T. Carrington, Chem. Phys. Lett. **287**, 289 (1998).
- ³⁹ See EPAPS Document No. E-JCPSA6-116-002217 for the calculated energy levels for H₃⁺ with *J*=0-15. This document may be retrieved via the EPAPS homepage (http://www.aip.org/pubservs/epaps.html) or from ftp.aip.org in the directory /epaps/. See the EPAPS homepage for more information.
- ⁴⁰B. M. Dinelli, L. Neale, O. L. Polyansky, and J. Tennyson, J. Mol. Spectrosc. **181**, 142 (1997).
- ⁴¹B. M. Dinelli, O. L. Polyansky, and J. Tennyson, J. Chem. Phys. **103**, 10433 (1995).
- ⁴²C. M. Lindsay and B. J. McCall, J. Mol. Spectrosc. **210**, 60 (2001).
- ⁴³ O. L. Polyansky, R. Prosmiti, W. Klopper, and J. Tennyson, Mol. Phys. 98, 261 (2000).
- ⁴⁴W. Meyer, P. Botschwina, and P. G. Burton, J. Chem. Phys. **84**, 891 (1986).
- ⁴⁵ M. Farnick, S. Davis, M. A. Kostin, O. L. Polyansky, J. Tennyson, and D. J. Nesbitt, J. Chem. Phys. (in press).
- ⁴⁶B. R. Johnson, J. Chem. Phys. **92**, 574 (1990).